Wavelet based separable analysis of texture images for extracting orientation of a planar surface

Sukhendu Das
School of Engineering
University of Applied Sciences
Tiefenbronner Str. 65,
D-75175, Pforzheim, Germany.
Email: sdas@fh-pforzheim.de

Thomas Greiner
School of Engineering
University of Applied Sciences
Tiefenbronner Str. 65,
D-75175, Pforzheim, Germany.
Email: TGreiner@fh-pforzheim.de

Abstract: The objective of this paper is to analyze the spectral variations of texture spatial frequencies as a function of orientation and depth of a 3-D planar surface. Based on this relationship we attempt to derive an expression for the extraction of 3-D surface orientation using texture features alone. Using experimentation on simulated images, we illustrate the advantage of using 1-D wavelets over Fourier based analysis for this purpose.

Key Words: Surface Reconstruction, texture, orientation, wavelet, spectral variations.

1. Introduction

The problem of obtaining 3-D surface orientation from a monocular static texture image has received a great of attention [1,2,7,8,10-16] in the field of computer vision and pattern recognition. If the surface exhibits a textured pattern, it is often easy for a human being to extract the structure information from the image. But the problem is ill-posed for a machine to solve. This paper presents analytical expressions using separable 1-D analysis of 2-D images for extraction of surface orientation of a textured planar surface.

In this paper we use a model of the viewing geometry which is similar to that used by Nayar et. al. [4-6] in Curet database [http://www.cs.columbia.edu/CAVE/curet/], but different from the one used by Super and Bovik [11], Ribeiro and Hancock [10] and Leung and Malik [14]. Dana [4] and Nayar [5] however used our proposed model of the viewing geometry for measurements of surface reflectance of textured surfaces, based of different viewing angles and illumination. Other work [3, 17] have concentrated on visualization of surfaces using 3-D textures. The work by Malik [14] used density, height and occlusion to derive the shape from textures. Super and Bovik [11], Ribeiro and Hancock [10] in their work have attempted to extract surface orientation using spectral gradient, peaks and distortion. Most of the earlier work [1, 7, 8, 11, 15, 16] involved an exhaustive numerical search. The most recent work [10] uses the eigenstructure of an affine distortion matrix. The advantage with our method will be the separable analysis in both dimensions of the image to extract the individual components of the surface orientation parameters. This will be evident in the next section, when we present the viewing geometry and derive the analytical expressions. Due to separable analysis, errors in computation of one of the orientation angles will not effect the other, which is a drawback in the method suggested in [10]. We then present the need and use of a multi-resolution filter (wavelet) for spectral analysis of texture surfaces to extract the surface orientation.

2. Basic projective texture equations

Figure 1. shows the viewing geometry and coordinate system used. Consider a surface element S, containing a simple sinusoidal texture. This simplicity is assumed to derive the relationship between spectral features of the texture pattern in the image space and 3-D surface properties (depth and surface orientation) of S.

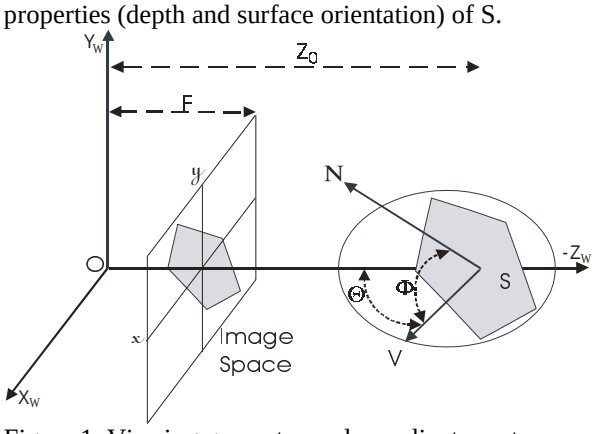

Figure 1. Viewing geometry and coordinate system.

Let N be the surface normal on S. This vector is defined using polar and azimuth angles of N w.r.t the world coordinate system. The azimuth angle ϕ, is the angle between the vector N and its projection, V, on the horizontal Z_W-X_W plane. The polar angle, θ (in the Z_W-X_W plane), is the angle between the vector V and Z_W axis, clock-wise looking along the Y-axis from the origin. This model is similar to that used in the CURET database [1]. The view axis is along the $-Z_W$ axis and F be the focal length of the viewing system, assuming a pin-hole camera configuration and perspective geometry of the viewing setup. The image plane (2-D) coordinate system is aligned with the X_W-Y_W axis of the world-coordinate system.

Assume a simple sinusoidal texture pattern on a planar surface with frequency f_r. Let the surface S be at a distance Z_0, from the origin. Let the surface inclination be such that either θ or ϕ is zero and the other be a non-zero value α. When $\theta = 0$, we do not have any local spectral variations along the x-axis (horizontal direction) of the image plane. Similarly, when $\phi = 0$, we do not have any local spectral variations along the y-axis (vertical direction) of the image plane.

When only one of the angles is non-zero (say, ϕ), and the other non-zero, the local spectral variations will be only along one of the principal axis (in this case, y-axis) of the image plane. Let the frequency content of the sinusoidal texture on a planar surface, at a distance Z_0 from the origin and oriented orthogonal to the viewing direction, as observed in the image space be a local spectral peak at f_r. Let f_r be assumed to be known initially (this constraints will be relaxed later on). Assume orthogonal projection initially, without any loss of generality. Perspective projection and effect of depth will be considered and incorporated next. If the surface is inclined such that, $\theta = 0$ and $\phi = \alpha$, then the observed frequency peak will be f_r', where

$$f_r' = f_r \sec(\alpha). \quad (1)$$

This relation is illustrated in figure 2. Eqn. (1) gives the relation between the observed frequency of the texture surface and inclination of the surface w.r.t. viewing direction. Thus if $\theta = \beta$ and $\phi = \alpha$, then the observed frequency will be,

$$f_r'' = f_r \sec(\beta). \sec(\alpha) \quad (2)$$

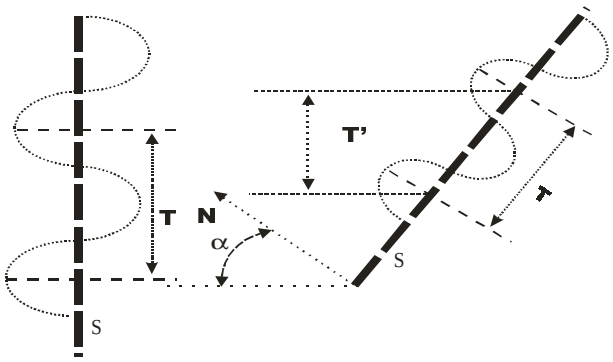

(a) (b)

Figure 2. (a) A simple sinusoid texture pattern on a planar surface S, oriented orthogonal to the viewing direction ($\theta = \phi = 0$). (b) The surface is oriented at $\phi = \alpha$ and $\theta = 0$. The projection of one period of the sinusoid is, $T' = T \cos(\alpha)$. Orthogonal projection is assumed and the sinusoidal texture pattern is shown as a dotted curve on the planar surface S.

Let us now observe the effect of depth of the surface from the viewer on the frequency peak. From figure 3(A), we can write using perspective projection models, the following equation:

$$H/Z_0 = h/F \quad (3)$$

where H is the time period of the sinusoid on the object surface, and h (= 1/ f_r) is the observed time period on the image plane. If the surface is moved away from the viewer by a distance ΔZ, then

$$H/Z' = h'/F \quad (4)$$

where $Z' = Z_0 + \Delta Z$, and h' is the observed time period of the sinusoid under perspective projection. Combining equations (3) and (4), we have:

$$h' = \frac{FH}{Z'} = \frac{FH}{(Z_0 + \Delta Z)} = \frac{FH}{Z_0(1 + \frac{\Delta Z}{Z_0})} = \frac{h}{1 + \frac{\Delta Z}{Z_0}} \quad (5)$$

The observed frequency, f_z, now is:

$$f_z = \frac{1}{h'} = \frac{1 + \frac{\Delta Z}{Z_0}}{h} = f_r(1 + \frac{\Delta Z}{Z_0}) \quad (6)$$

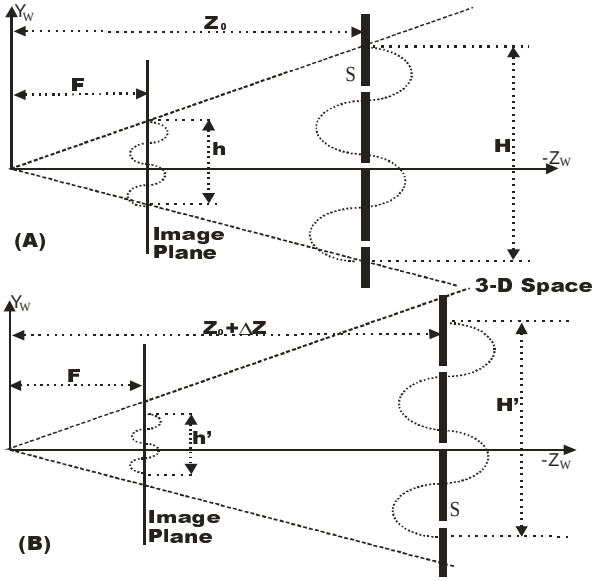

Figure 3. The planar surface, S, oriented orthogonal to the viewing direction, is projected on the image plane. (A) Surface is at a distance Z_0 from the camera and length of the projected segment is h. (B) Surface is now at a distance ($Z_0 + \Delta Z$) from the camera and the length of the projected segment is h'. F is the focal length of the camera and viewing direction is along the $-Z_w$ axis.

From equations (2) and (6), we get the locally observed frequency f_{oi}, of a planar surface at depth ($Z_0 + \Delta Z_i$), and orientation $\theta = \beta$, $\phi = \alpha$, as:

$$f_{oi} = f_r(1 + \frac{\Delta Z_i}{Z_0})(\sec\alpha)(\sec\beta) = f_r(\frac{Z_i}{Z_0})(\sec\alpha)(\sec\beta) \quad (7)$$

where, $Z_i = Z_0 + \Delta Z_i$.

Equation 7 is the basic equation for the observed texture frequency in the image plane, depending on the surface parameters (depth ($Z_0 + \Delta Z_i$) and orientation α, β). The plot in Figure 4, illustrates the nature of the frequency variation, given in equation (7), where the normalized observed frequency is (f_{oi}/f_r).

If any texture pattern can be considered as a superposition of several sinusoids (band-limited), then all the individual components of the signal will also be effected in a similar manner as in equation (7). We will now derive equations which estimate the surface orientation parameters from the observed frequency f_{oi}, on the image plane. Henceforth, the term 'frequency' will mean the observed local spectral peak of the texture around a neighborhood of a point in the image plane.

3. Estimation of orientation parameters

Observe Figure 5, which shows the perspective geometry of a planar surface S inclined at an angle $\phi = \alpha$ and $\theta = 0$. Select two points I and J, on the vertical axis on the image plane, with coordinates (x_i, y_i) and (x_i, y_j) respectively. These may be considered to be the projections, on the image plane, of points P_i and P_i on S.

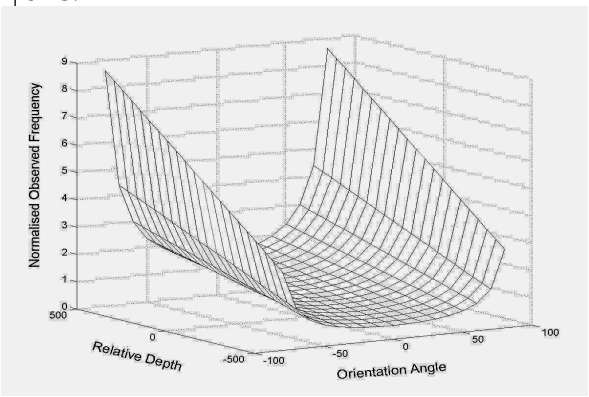

Figure 4. Normalized observed frequency (f_{oi}/f_r), in the image texture pattern, as a function of relative depth ΔZ_i and orientation angle α.

In equation(7), substituting $\phi = \alpha$ and $\theta = 0$, we have:

$$f_{oi} = f_r(1+\frac{\Delta Z_i}{Z_0})(\sec\alpha)$$, at a point (x_i, y_i) in the image plane, and

$$f_{oj} = f_r(1+\frac{\Delta Z_j}{Z_0})(\sec\alpha)$$, at a point (x_i, y_j) in the image plane.

Since the polar angle $\theta = 0$, the spectral gradient along the horizontal (x) axis of the image is zero. Hence we look for the variations in spectral values along the vertical (y) axis of the image plane. This role is reversed if $\phi = 0$ and $\theta = \beta$. From the above two equations, we can obtain the difference in the observed frequencies as:

$$\Delta f_o^{i,j} = f_{oj} - f_{oi} = f_{r\alpha}\frac{\Delta Z_{ij}}{Z_0} \quad (8)$$

where, $\Delta Z_{ij} = Z_j - Z_i$ ($= \Delta Z_j - \Delta Z_i$),
and $f_{r\alpha} = f_r(\sec\alpha)$.

For the ratio of the observed frequencies, we have:

$$f_{o(i,j)} = \frac{f_{oj}}{f_{oi}} = \frac{Z_0 + \Delta Z_j}{Z_0 + \Delta Z_i} = \frac{Z_j}{Z_i} = 1 + \frac{\Delta Z_{ij}}{Z_i} \quad (9)$$

Using perspective geometry, we write:

$$\Delta Z_{ij} = Z_j - Z_i = F[\frac{Y_j}{y_j} - \frac{Y_i}{y_i}]$$
$$= F[\frac{Y_i + \Delta Y_{ij}}{y_i + \Delta y_{ij}} - \frac{Y_i}{y_i}] = F[\frac{y_i\Delta Y_{ij} - Y_i\Delta y_{ij}}{y_i(y_i + \Delta y_{ij})}] \quad (10)$$

where $\Delta Y_{ij} = Y_j - Y_i$ (3-D world space coordinates)
and $\Delta y_{ij} = y_j - y_i$ (2-D image plane coordinates).

From figure 5, we can write:

$$\Delta Y_{ij} = \Delta Z_{ij}(\cot\alpha)$$

and with some simplifications, we can derive (see Appendix A) from equation (10):

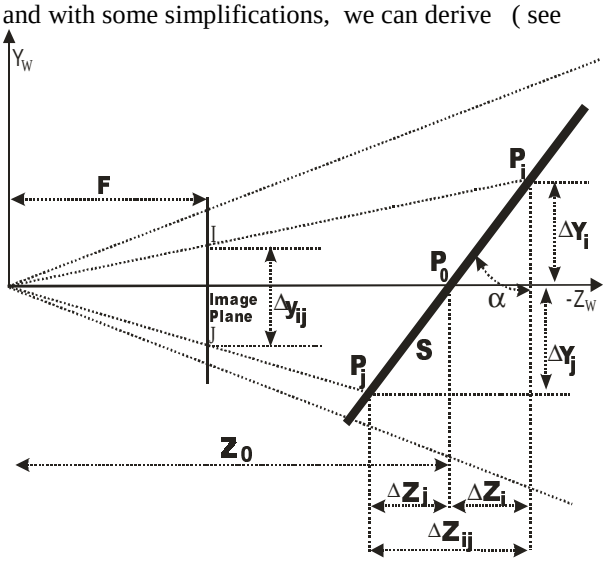

Figure 5. Surface S is oriented at an angle $\phi=\alpha$. Two points I and J, selected on the image plane correspond to points P_i and P_j on the surface. The viewing axis intersects the surface at P_0, with depth Z_0. The image plane is orthogonal to the view direction, and is viewed in the figure as a line.

$$\frac{\Delta Z_{ij}}{Z_i} = \frac{\Delta y_{ij}}{F(\cot\alpha) - y_j} \quad (11)$$

Substituting (11) in (9), we have

$$f_{o(i,j)} = 1 + \frac{\Delta Z_{ij}}{Z_i} = \frac{F(\cot\alpha) - y_j + (y_j - y_i)}{F(\cot\alpha) - y_j}$$
$$= \frac{F - y_i(\tan\alpha)}{F - y_j(\tan\alpha)} \quad (12)$$

Figure 6 below illustrates the variation in the ratio of the observed frequencies at two image coordinates Y_j and Y_i in the image planes as a function of orientation angle α and image coordinate Y_j ($= -Y_i$).

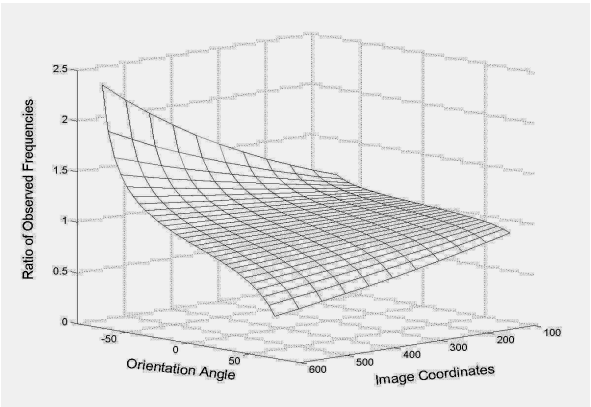

Figure 6. Ratio of the observed frequencies as a function of orientation angle α and image coordinate.

Equation (12) gives the relation between the ratio, $f_{o(i,j)}$, of the observed frequencies at two arbitrary points on a vertical line in the image plane and the orientation angle α. F can be normalized to unity or the image coordinates calibrated w.r.t. F.

Under the condition $y_j = 0$ (i.e. $Z_j = Z_0$, $\Delta Z_j = 0$, $\Delta Z_{ij} = Z_0 - Z_i = -\Delta Zi$ and $f_{oj} = f_{r\alpha}$), equations (12) and (9) give:

$$f_{o(i,o)} = \frac{f_{r\alpha}}{f_{oi}} = \frac{Z_0}{Z_i} = 1 - \frac{y_i(\tan\alpha)}{F} \quad (13)$$

From equation (13):

$$f_{oi} = f_{r\alpha}[\frac{F}{F - y_i(\tan\alpha)}] \quad (14)$$

Equation (14) gives the spectral frequency at a point (x_i, y_i), on the image plane, as a function of y_i, α and $f_{r\alpha}$ (frequency at y = 0).

Equation (8) gives us the numerical difference between the two observed frequencies, f_{oi} and f_{oj}, as:

$$\Delta f_o^{i,j} = f_{oj} - f_{oi} = f_{r\alpha}\frac{\Delta Z_{ij}}{Z_0}$$

Using the above equation along with (13), gives us:

$$\begin{aligned}\Delta f_o^{i,j} &= f_{oj} - f_{oi} \\ &= f_{r\alpha}[\frac{F}{F - y_j(\tan\alpha)} - \frac{F}{F - y_i(\tan\alpha)}] \\ &= Ff_{r\alpha}[\frac{(y_j - y_i)\tan\alpha}{(F - y_j\tan\alpha)(F - y_i\tan\alpha)}] \\ &= f_{oi}[\frac{(y_j - y_i)\tan\alpha}{F - y_j(\tan\alpha)}] = f_{oj}[\frac{(y_j - y_i)\tan\alpha}{F - y_i(\tan\alpha)}]\end{aligned} \quad (15)$$

Equations (12) and (15) give the same solution for the azimuth angle $\phi = \alpha$. This is given as (for derivation, see Appendix B):

$$\alpha = \arctan[\frac{F(f_{oj} - f_{oi})}{f_{oj}y_j - f_{oi}y_i}] = \arctan[\frac{F(f_{o(i,j)} - 1)}{f_{o(i,j)}y_j - y_i}] \quad (16)$$

Similarly, selecting a pair of points, (x_i, y_i) and (x_j, y_i), on a horizontal axis of the image plane, we obtain the polar angle $\theta = \beta$, as:

$$\beta = \arctan[\frac{F(f_{oj} - f_{oi})}{f_{oj}x_j - f_{oi}x_i}] = \arctan[\frac{F(f_{o(i,j)} - 1)}{f_{o(i,j)}x_j - x_i}] \quad (17)$$

Equations (16, 17) gives the solution for the orientation of the texture surface S, as a function of local spectral frequency and spatial coordinates of two points selected on the corresponding axis of the image plane. The advantage of the proposed method is the separable analysis in x and y directions which give the polar and azimuth angles of the surface orientation respectively.

The depth information (up to a scale factor [2, 9], in the absence of any additional information) can also retrieved using the analytical expressions derived so far (see equations 9-11). In the next section, we illustrate the advantage of using wavelet transform in detecting spectral differences in texture images with experimentation on simulated data.

4. Wavelet transform for 3-D texture analysis

Let us consider two 1-D signals obtained by scanning along the vertical lines of two texture images, of the same texture surface with varying posture. The images are illustrated in Figure 7. The images are simulated as a superimposition of two pure sinusoidal patterns. Typical plots (signal I and signal II) of the vertical scan lines of the pair of images in figure 7, are given in figure 8. The corresponding spectral plots are shown in figure 9, from which it can be observed that it is difficult to process the texture images using only the spectral peaks [7, 10, 11]. Hence it is necessary to use a multi-rate and multi-resolution filter bank to discriminate these features, rather than the use of a simple Fourier based analysis.

We suggest the use of wavelet transform for this purpose. The wavelet plots for the signals in figure 8, are shown in figure 10 (detail coefficients at level 1 are not shown, as the values are negligible). Daubechies 10-tap filter [18] with 3 levels of decomposition is used for this purpose. The wavelet features exhibit a distinct difference in the response noticeably at detail levels 2 and 3, unlike the Fourier spectral features (compare the pair of plots in figures 9 and 10). The process of energy computation from the wavelet coefficients consists of two steps. The first step involves mean subtraction, squaring and Gaussian smoothing. This post-processed signal is illustrated in figure 11, which is obtained from the 1-D wavelet coefficients shown in figure 10. The second step involves computing the variances of the post-processed signal in figure 10, for each level of decomposition separately (namely, A3, D3 and D2).

We have observed that the sum of the weighted (empirically obtained) differences of the variances of the energy levels in the corresponding bands of the wavelet decomposition is related to the orientation angle and depth of the surface, as illustrated in figures 4 and 6. To compute the orientation of the surface, using equations (16) & (17), the ratio of the observed frequencies, $f_{o(i,j)}$, is computed using an identical ratio of the weighted sums of the variances. Issues of accuracy and experimentation with real world data are beyond the scope of this paper.

5. Conclusion

This paper illustrates the advantage of wavelet transform for discriminating two texture images with varying orientation (in 3-D). This method is superior than the other spectral based methods used in [7, 8, 10, 11, 12 – 17]. The difference of the energy levels in the decomposition bands, can be used to obtain the orientation of the texture surface. Expressions relating the orientation and depth of a texture surface with the spectral contents of the image texture have been

derived. The spectral variations are less sensitive (and hence errors are large) when the surface orientation and image resolution are small. Results are shown using experimentation with simulated data.

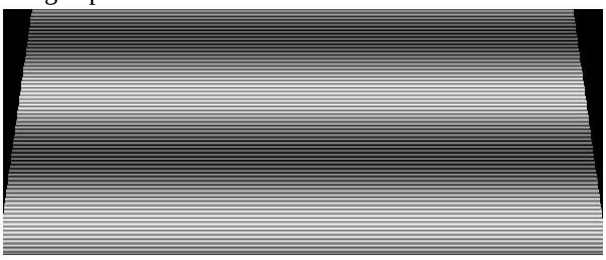

(a) Simulated Texture Image I

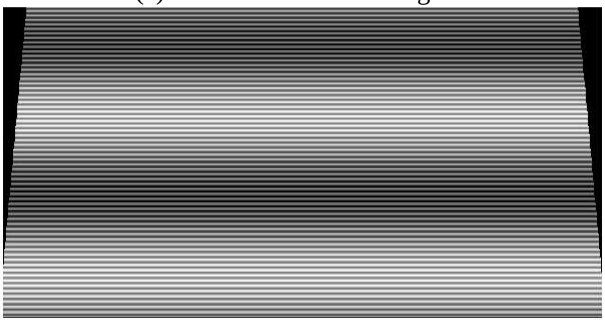

(b) Simulated Texture Image II

Figure 7. Two texture images of the same surface with a difference in only one of the orientation angles.

Appendix A

Using perspective geometry, equation (10):

$$\Delta Z_{ij} = Z_j - Z_i = F[\frac{Y_j}{y_j} - \frac{Y_i}{y_i}] \\ = F[\frac{Y_i + \Delta Y_{ij}}{y_i + \Delta y_{ij}} - \frac{Y_i}{y_i}] = F[\frac{y_i \Delta Y_{ij} - Y_i \Delta y_{ij}}{y_i (y_i + \Delta y_{ij})}] \quad (A.1)$$

From figure 5 we have the relation,

$$\Delta Y_{ij} = \Delta Z_{ij} (\cot \alpha)$$

Hence from equation (A.1),

$$\Delta Z_{ij} (y_i^2 + y_i \Delta y_{ij}) = F[y_i \Delta Z_{ij} (\cot \alpha) - Y_i \Delta y_{ij})]$$

Using $\Delta y_{ij} = y_j - y_i$, we then have :

$$\Delta Z_{ij} (y_i y_j - F y_i \cot \alpha) = -F Y_i \Delta y_{ij} = -F (\frac{y_i Z_i}{F}) \Delta y_{ij}$$

$$\frac{\Delta Z_{ij}}{Z_i} = -\frac{\Delta y_{ij} y_i}{y_i y_j - F y_i \cot \alpha} = \frac{\Delta y_{ij}}{F \cot \alpha - y_j}$$

Appendix B

From equation (15), we have

$$\Delta f_o^{i,j} = f_{oj} - f_{oi} = f_{oi} [\frac{(y_j - y_i) \tan \alpha}{F - y_j (\tan \alpha)}]$$

Thus

$$\tan(\alpha)[f_{oi} (y_j - y_i)] = \Delta f_o^{i,j} [\mathrm{F} - y_j (\tan \alpha)]$$

Hence

$$\tan(\alpha) = \frac{\Delta f_o^{i,j} F}{f_{oi} (y_j - y_i) + y_j (f_{oj} - f_{oi})} \\ = \frac{\mathrm{F} (f_{oj} - f_{oi})}{f_{oj} y_j - f_{oi} y_i}$$

REFERENCES

[1] B. K. P. Horn and M. J. Brooks, Shape from shading, MIT Press, 1989.

[2] Y. Shirai, Three-dimensional Computer Vision, Springer-Verlag, 1987.

[3] P. Suen and G. Healey, The analysis and recognition of real-world textures in three-dimensions, IEEE Transactions on Pattern Analysis and Machine Intelligence, Vol. 22, No. 5, May 2000, pp 491-503.

[4] K. J. Dana, S. K Nayar, B. V. Ginneken and J. Koenderink, Reflectance and texture of real-world surfaces, Proceedings of the CVPR, June1997, pp 151-157.

[5] S. K. Nayar, K. Ikeuchi and T. Kanade, Surface reflection: physical and geometric perspectives, IEEE Transactions on Pattern Analysis and Machine Intelligence, Vol. 13, No. 7, July 1991, pp 611-634.

[6] M. Oren and S. K. Nayar, Generalization of the Lambertian model and implications for machine vision, International journal of Computer Vision, Vol. 14, 1995, pp 227-251.

[7] B. J. Super and A. C. Bovik, Shape from Texture using local spectral moments, IEEE Transactions on Pattern Analysis and Machine Intelligence, Vol. 17, No. 4, April 1995, pp 333-343.

[8] Y. Choe and R. L. Kashyap, 3-D shape from a shaded and textural surface image, IEEE Transactions on Pattern Analysis and Machine Intelligence, Vol. 13, No. 9, September 1991, pp. 907-919.

[9] Y. Jiang and H. Bunke, Dreidiemsionales Computersehen, Springer Verlag, 1997.

[10] Eraldo Ribeiro and Edwin R. Hancock, Shape from periodic Texture using the eigenvectors of local affine distortion, IEEE Transactions on Pattern Analysis and Machine Intelligence, Vol. 23, No. 12, Dec. 2001, pp 1459 – 1465.

[11] B. J. Super and A. C. Bovik, Planar surface orientation from texture spatial frequencies, Pattern Recognition, Vol. 28, No. 5, 1995, pp 729-743.

[12] J. S. Kwon, H. K. Hong and J. S Choi, Obtaining a 3-D orientation of Projective textures using a Morphological Method, Pattern Recognition, Vol. 29, 1996, pp 725-732.

[13] J. V. Stone and S. D. Isard, Adaptive Scale Filtering: A general method for obtaining shape from Texture, IEEE Transactions on Pattern Analysis and Machine Intelligence, Vol. 17, No. 7, July 1995, pp 713-718.

[14] Thomas leung and Jitendra Malik, On Perpendicular textures, or: Why do we see more flowers in the distance?, Proceedings of the IEEE Conference on Computer Vision and Pattern Recognition (CVPR '97), 1997, pp 807-813.

[15] Jonas Garding, Surface Orientation and Curvature from Differential Texture Distortion, Proceedings of the IEEE Conference on Computer Vision (ICCV '95), 1995, pp 733-739.

[16] Peter N. Belhumeur and Alan L. Yuille, Recovering Object Surfaces from Viewed changes in Surface Texture Patterns", Proceedings of the IEEE Conference on Computer Vision (ICCV '95), 1995, pp 876-881.

[17] Victoria Interrante, Henry Fuchs and Stephen M. Pizer, Conveying the 3-D shape of smoothly curving Transparent Surfaces via Texture, IEEE Transactions on Visualization and Computer Graphics, Vol. 3, No. 2, April-June 1997, pp 98-117.
[18] I. Daubechies, Wavelets, Philadelphia, Pa.: S.I.A.M., 1992.

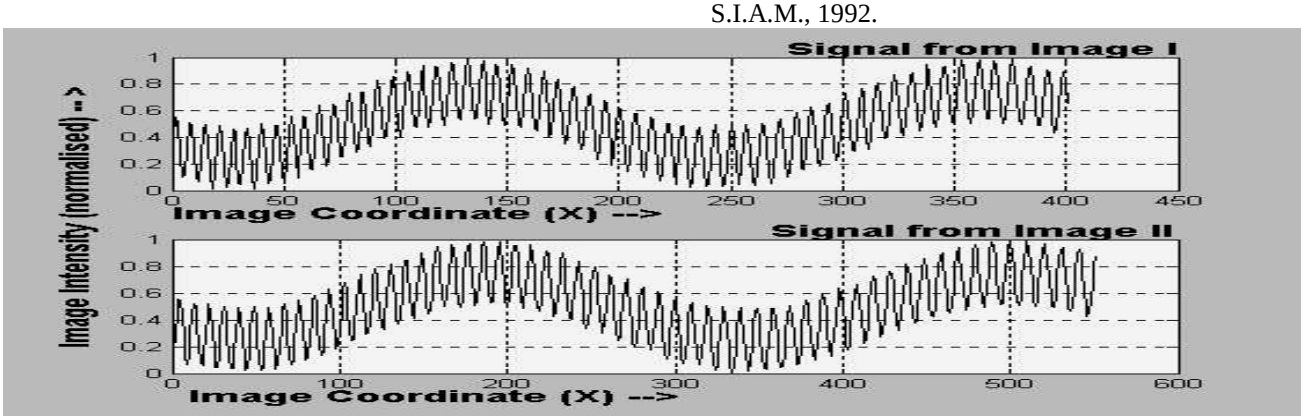

Figure 8. Intensity profiles along a vertical scan line of the images shown in figure 7.

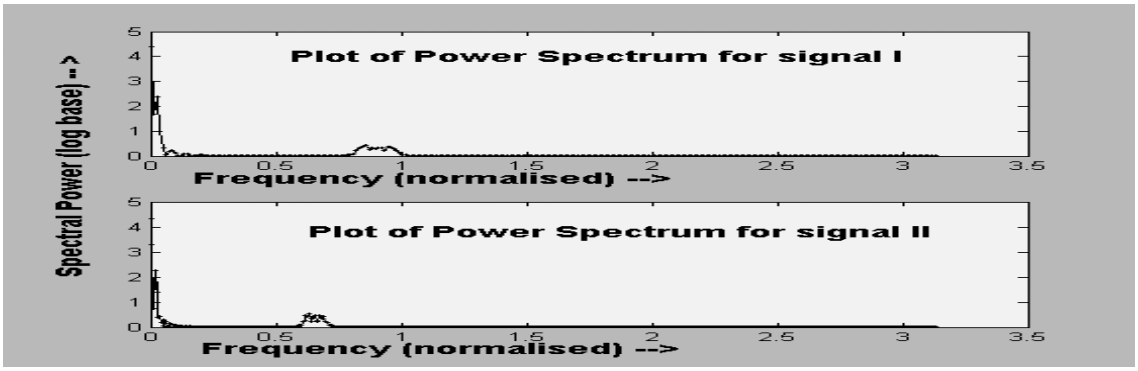

Figure 9. Plots of the log spectral power for the corresponding 1-D intensity profiles in figure 8.

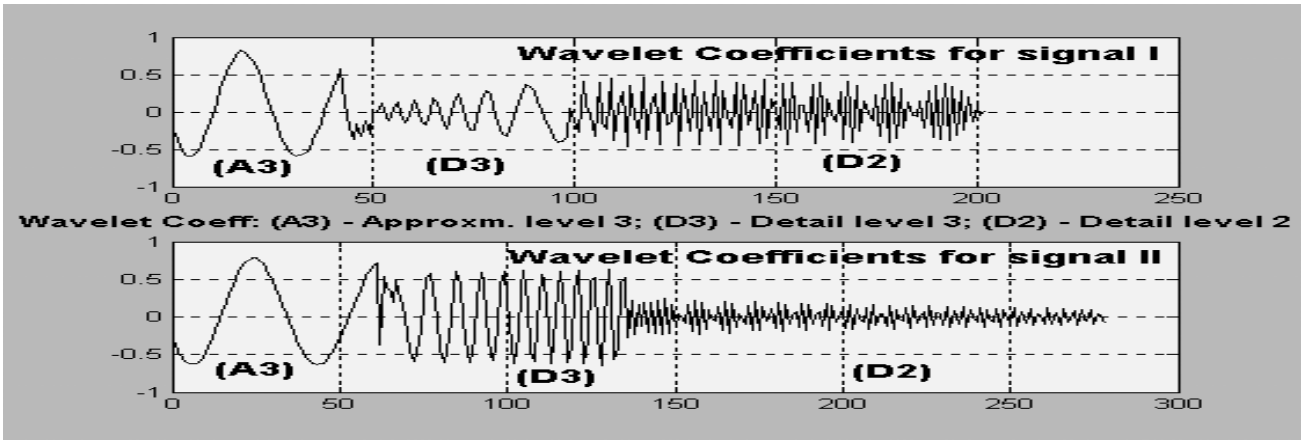

Figure 10. Wavelet coefficients (level 3 decomposition) of the corresponding pair of signals shown in figure 8.

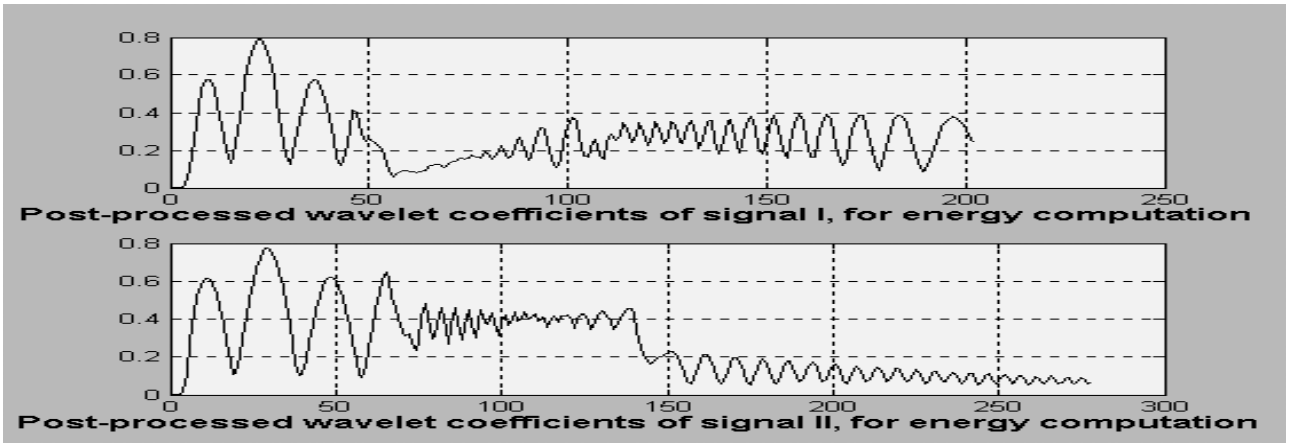

Figure 11. Energy features at the corresponding levels derived from the wavelet coefficients